Published in final edited form as:
J Child Neurol. 2009 September ; 24(9): 1179–1189. doi:10.1177/0883073809338213.

Intrauterine Endotoxin Administration Leads to White Matter Diffusivity Changes in Newborn Rabbits

Fadoua Saadani-Makki, PhD, **Sujatha Kannan, MD**, **Malek Makki, PhD**, **Otto Muzik, PhD**, **James Janisse, PhD**, **Roberto Romero, MD**, and **Diane Chugani, PhD**
Carman and Ann Adams Department of Pediatrics (FS-M, SK, OM, DC), Departments of Radiology (MM, OM, DC), Medicine (JJ) and Molecular Medicine and Genetics (RR), Wayne State University School of Medicine, Detroit, Michigan, and the Perinatology Research Branch, Department of Health and Human Services, National Institute of Child Health and Human Development, National Institutes of Health (RR).

Abstract

Maternal intrauterine inflammation has been implicated in the development of periventricular leukomalacia and white matter injury in the neonate. We hypothesized that intrauterine endotoxin administration would lead to microstructural changes in the neonatal rabbit white matter in vivo that could be detected at birth using diffusion tensor magnetic resonance imaging (MRI). Term newborn rabbit kits (gestational age 31 days) born to dams exposed to saline or endotoxin in utero on gestational day 28 underwent diffusion tensor imaging, and brain sections were stained for microglia. Comparison between normal and endotoxin groups showed significant decreases in both fractional anisotropy and eigenvalue (e_1) in all periventricular white matter regions that showed an increase in the number of activated microglial cells, indicating that after maternal inflammation, microglial infiltration may predominantly explain this change in diffusivity in the immediate neonatal period. Diffusion tensor imaging may be a clinically useful tool for detecting neuroinflammation induced by maternal infection in neonatal white matter.

Keywords

periventricular leukomalacia; cerebral palsy; neuroinflammation; diffusion tensor imaging; fractional anisotropy; intrauterine inflammation; microglia; New Zealand white rabbits

White matter injury, in particular periventricular leukomalacia, is considered the leading cause of long-term neurological disorders underlying cerebral palsy. A growing body of evidence suggests that in addition to hypoxic-ischemic injury, intrauterine infection or inflammation plays a central role in the etiology of periventricular leukomalacia and cerebral palsy.[1-7] Conventional magnetic resonance imaging (MRI) has been widely considered the neuroanatomical imaging tool of choice in detecting brain lesions in the neonatal period and in children with cerebral palsy. It has been used to reveal macrostructural brain abnormalities such as periventricular leukomalacia, ventricular enlargement, proencephalic cysts, and cerebral atrophy.[8-11] However, conventional MRI has

Address correspondence to: Sujatha Kannan, Children's Hospital of Michigan, Carman & Ann Adams Department of Pediatrics, Wayne State University, 3901 Beaubien Blvd., Detroit, MI 48201; skannan@ med.wayne.edu..

The authors have no conflicts of interest to disclose with regard to this article.

Saadani-Makki F, Kannan S, Makki M, et al. Intrauterine endotoxin administration leads to white matter diffusivity changes in newborn rabbits. *J Child Neurol*. 2009;24:1179-1189.

failed to detect micropathology in patients with cerebral palsy.[12,13] Recently, Korzeniewski and colleagues reported that 17% of these patients have no abnormality detectable by conventional MRI.[14] Thus, newer MRI techniques, including diffusion tensor and diffusion-weighted imaging, perfusion MRI, magnetic resonance spectroscopy, and functional MRI, may provide more detailed information at the structural and functional level.

Diffusion tensor imaging is a noninvasive MRI technique based on the measurement of random displacement of water molecules. It allows an assessment of white matter integrity in different diseases. In white matter, fibers are oriented in bundles, and water molecules diffuse more freely along the direction of the fibers but are restricted in their movement perpendicular to the fibers. This directionally dependent diffusion is termed anisotropic diffusion and is directly proportional to fiber density and inversely related to membrane permeability. Tissue diffusion is characterized by the apparent diffusion coefficient, providing a measure of overall magnitude of water diffusion independent of anisotropy, and by fractional anisotropy, an indicator of the degree of anisotropic diffusion.[15,16] The apparent diffusion coefficient and fractional anisotropy parameters are well-established measures of micro-structural abnormality otherwise not detectable by conventional MRI. Diffusion tensor imaging has been used to assess cerebral white matter abnormalities in preterm and term infants and in children with periventricular leukomalacia and cerebral palsy.[12,13,15,17] In these patients, a decrease in fractional anisotropy was noted in the white matter regions, suggestive of damage to the fiber tracts or impairment in their subsequent development.

Several animal studies using diffusion-weighted MRI to evaluate brain injury after hypoxic-ischemia in neonatal mice[18] and rats[19] have shown a decrease in the apparent diffusion coefficient in the brain tissue. Drobyshevsky and colleagues, using diffusion tensor imaging, have demonstrated that newborn rabbits with hypertonia secondary to hypoxic-ischemic insult in utero had a decrease in fractional anisotropy in the corpus callosum and internal capsule *that corresponded with a decrease* in the number and density of fiber tracts.[20] We have previously established a rabbit model of intrauterine inflammation that leads to a phenotype of cerebral palsy in the neonate, with microglial infiltration in the immediate newborn period (postnatal day 1) and hypomyelination at postnatal day 5.[21,22] We hypothesized that maternal intrauterine endotoxin administration leads to changes in water diffusivity in the periventricular white matter regions in the newborn rabbit.

Materials and Methods

Animal Model

All the animal experimental procedures were approved by the Animal Investigation Committee of Wayne State University and were conducted in strict compliance with the policies of the animal welfare and care of the National Institute of Health and Wayne State University. The details of the surgical procedures were described previously by our group.[21] Briefly, New Zealand White rabbits (Covance Research Products Inc, Kalamazoo, Michigan) with timed pregnancies that were confirmed breeders with a history of delivering 7 to 11 kits per litter underwent laparotomy under general anesthesia (2% to 3% isoflurane by mask) on gestational day 28 (E28, term pregnancy is 31 to 32 days). One milliliter of saline in the control group (n = 5) and 1 mL of saline containing 20 μg/kg of lipopolysaccharide (*Escherichia coli* serotype 0127:B8; Sigma-Aldrich, St Louis, Missouri) in the endotoxin group (n = 5) were injected into the uterine wall using a 27-gauge needle between the fetuses, taking care not to enter the amniotic sac. This ensured that all the kits were exposed to the same amount of endotoxin. Normothermia was maintained using a water-circulating blanket, and heart rate, oxygen saturations, and arterial blood pressure measured through a 20-gauge arterial catheter placed in the marginal ear artery were

monitored continuously during the procedure. A surveillance camera was placed in the rabbit room and the dams monitored remotely to determine the time of delivery. The kits were born spontaneously at 31 days' gestational age with a phenotype of cerebral palsy in the endotoxin kits, as described previously by our group.[22] The litter size ranged from 7 to 12 kits and 1 to 2 kits from each litter underwent MRI scanning, including diffusion tensor imaging protocol.

Diffusion Tensor Imaging Protocol

Before MRI acquisition, postnatal day 1 rabbits were anesthetized with isoflurane (2% isoflurane was used for induction and 0.2 % for maintenance) and were kept warm during the MRI scan using a water-circulating blanket at 37° C. Rectal temperature was monitored continuously with a fiberoptic thermometer (Luxtron, Santa Clara, California) and normothermia maintained for all rabbits. Heart rate and oxygen saturations were monitored throughout the procedure. A special customized head and body holder was designed that enabled immobilization of the head and body in a prone position. The head was placed in a slightly elevated position to minimize interference due to respirations.

Brain images were acquired on a small-animal Bruker Biospec-Avance 4.7 T horizontal-bore magnet (gradient = 200 mT/m, rise time = 170 microsecond) using a surface coil. Diffusion tensor images were acquired using a spin-echo sequence with diffusion sensitizing gradients of b = 800 (s/mm^2) applied in 6 noncol-linear directions [(x, y, z) = (0.707, 0.707, 0) (0.707, –0.707, 0) (0.707, 0, 0.707), (–0.707, 0, 0.707), (0, 0.707, 0.707) (0, 0.707, –0.707)] and a reference T2-weighted scan (b = 0 (s/mm^2)]. Imaging parameters were as follows: repetition time = 4000 milliseconds, echo-time = 37 milliseconds, field-of-view = 32 × 32 mm, matrix size 128 × 128, slice thickness = 0.7 mm (no gap), and acquisition time ~40 minutes. Eight contiguous slices were acquired with the first slice selected at the level of the bregma (Figure 1).

Diffusion tensor imaging metrics were measured using the DTIStudio software,[23] yielding the 3 diffusion tensor eigenvalues (e_1, e_2, e_3, units of mm^2/s) characterizing the 3 axes of the diffusion ellipsoid. Moreover, parallel (along fiber direction) diffusivity was characterized by the main eigenvalue (e_1), whereas water diffusivity perpendicular to axonal fibers was described by the mean of the 2 minor eigenvalues (e_3, e_2). Lastly, the apparent diffusion coefficient (ADC, units of mm^2/s) was calculated as the mean of all 3 eigenvalues, and the fractional anisotropy (FA, unitless) was calculated based on the following equations:

$$e_{23}=\frac{e_2+e_3}{2}\left(\mathrm{mm}^2/\mathrm{s}\right),\quad \mathrm{ADC}=\frac{e_1+e_2+e_3}{3}\left(\mathrm{mm}^2/\mathrm{s}\right),$$
$$\mathrm{FA}=\sqrt{\frac{3}{2}}\sqrt{\frac{(e_1-\mathrm{ADC})^2+(e_2-\mathrm{ADC})^2+(e_3-\mathrm{ADC})^2}{e_1^2+e_2^2+e_3^2}} \quad (1)$$

A directional color-encoded map was created from the orientation of the main eigenvalue using the combination of red-green-blue colors. Fibers oriented left-right were encoded in red, those oriented dorsoventral in green, and those encoded oriented craniocaudal in blue (Figure 1). Studied structures included the corpus callosum, internal capsule (bilaterally), anterior commissure, corona radiata (bilaterally), and hippocampus (bilaterally). These structures were manually delineated by drawing regions of interest on the directionally color-encoded map, in all slices that contained the structures (Figure 1). Care was taken to include as much pixels as possible for each structure while avoiding partial volume effects.

Immunohistochemistry

After the MRI, rabbit kits were perfused intracardiac on the same day with 4% paraformaldehyde under deep anesthesia. Their brains were removed and immersed in the

same fixative for 48 hours, cryoprotected using graded solutions of sucrose, and frozen at –800° C until they were sectioned. Thirty-micrometer thick coronal brain sections were cut using a cryostat (Leica Microsystems, Nuchloss, Germany) and mounted on poly-L-lysine-coated slides (Sigma-Aldrich).

For immunohistochemical staining, sections were rinsed in phosphate-buffered saline and treated with ethanol for 35 minutes to inactivate endogenous peroxidase. The sections were permeabilized for 1 hour with phosphate-buffered saline containing 0.3% triton X-100 and 0.5% bovine serum albumin. The sections were incubated for 1 hour with biotinylated *Lycopersicon esculentum* tomato lectin (1:100 dilution in phosphate-buffered saline containing 0.3% triton X-100/bovine serum albumin; Vector Laboratories, Burlingame, California) for microglial staining, or mouse monoclonal Pan-axonal neuro-filament marker (SMI-312, 1/50 dilution in phosphate-buffered saline containing 0.3% triton X-100/bovine serum albumin; Covance, Emeryville, California) for phosphorylated neurofilaments, respectively. After incubation, the sections used for neurofilament staining were rinsed in phosphate-buffered saline containing 0.3% triton X-100/phosphate-buffered saline and incubated for 2 hours at room temperature with biotinylated goat anti-mouse immunoglobulin G (1:250 dilution in phosphate-buffered saline containing 0.3% triton X-100/bovine serum albumin; Vector Laboratories) as secondary antibody. Avidin binding was done using Vectastain ABC kit according to manufacturer instructions, and color developed using 3,3′-diaminobenzidine as a peroxidase substrate (Vector Laboratories). Sections were then rinsed in phosphate-buffered saline, dehydrated in graded ethanol, and cleared in xylene. For all staining, sections were mounted with mounting medium (Electron Microscopy Sciences, Hatfield, Pennsylvania) and viewed using a Leica DM2500 microscope (Leica Microsystems) equipped with a camera.

The staining of microglial cells was performed on every fourth section extending from the level of the bregma. Microglial cells in 3 representative white matter regions, the corpus callosum, anterior commissure, and internal capsule (bilaterally), were counted. On each section, 6 images were captured at × 40 magnification (total area of 0.54 mm^2) to cover the totality of the structure. On the basis of morphology, the microglia were classified as ramified (resting) or bushy and round (activated), as described previously (Figure 2).[21] The ratio of the activated cells (bushy and round cells) compared with total number of microglial cells (ramified + bushy and round) was calculated and compared for the control and endotoxin groups. The ratio of activated to total microglia for each rabbit was also correlated with its fractional anisotropy, apparent diffusion coefficient, and directional diffusivities (e_1 and e_{23}) measured in the corpus callosum, anterior commissure, and internal capsule.

Statistical Analysis

Prior to the analyses, distributions of all outcome variables were examined for accuracy and outliers. For analysis of the diffusion tensor imaging parameters, all slices that represented each of the structures was included. For bilateral structures such as the internal capsule, corona radiata, and hippocampus, data obtained from the left and right hemisphere were averaged. To compare the 2 groups (control, endotoxin) with respect to diffusion tensor imaging parameters while taking into account repeated measurements as well as nesting of some of the pups within litters, a generalizing estimating equations approach was used. A first-order autoregressive correlation structure was used to represent the within-subject dependencies among the variables. Data were expressed as mean with 95% confidence intervals obtained from the generalizing estimating equations. The ratio of activated to total microglial cells between the groups was analyzed using a t test and expressed as mean and standard deviation.

Results

Analyses of Diffusion Tensor Imaging Parameters

Diffusion tensor images were obtained according to the protocol described on 5 kits from 4 litters in the control group and 5 kits from 3 litters in the endotoxin group. A significant decrease in e_1 resulting in a decrease of fractional anisotropy was observed in the endotoxin group compared with the control group in periventricular white matter, including the corpus callosum, anterior commis-sure, internal capsule, and corona radiata (Table 1). Based on the analysis of the parallel (e_1) and perpendicular (e_{23}) diffusivities, it appears that the decrease in fractional anisotropy in the periventricular white matter regions of lipopolysaccharide-exposed kits is mainly caused by the decrease in e_1. A tendency toward increase in e_{23} was observed in these regions and reached significance only in the region of the anterior commissure. There was no significant difference in the apparent diffusion coefficient in any periventricular region between the 2 groups (see Table 1). In the grey matter region (hippocampus), a significant decrease in both e_1 and e_{23}, resulting in a decrease in apparent diffusion coefficient, was observed in the endotoxin group. In contrast, no significant difference in the fractional anisotropy was noted between the 2 groups in the hippocampus (Table 1).

Immunohistochemistry

The presence of activated microglia was demonstrated by tomato lectin staining. Strong microglial activation was detected in the endotoxin kits compared with controls, as determined by an increase in the number and change in the morphology of the microglial cells to a less-ramified form with a larger cell body. This was noted in the corpus callosum; along the lateral ventricle; in the regions of internal capsule, corona radiata, and anterior commis-sure; and in the hippocampus (Figure 3). There was a significant increase in the ratio of activated cells compared with total number of microglial cells in the endotoxin kits when compared with controls, in all 3 regions (corpus callosum, mean ± SD was 0.34 ± 0.05 for the control and 0.81 ± 0.13 for the endotoxin group; $P < .005$; anterior commissure, mean ± SD was 0.13 ± 0.05 for the control and 0.71 ± 0.17 for the endotoxin group; $P < .005$; and internal capsule, mean ± SD was 0.34 ± 0.05 for the control and 0.84 ± 0.10 for the endotoxin group; $P < .005$; Figure 4).

Relationship Between Diffusion Tensor Imaging Parameters and Immunohistochemistry

To determine whether the decrease in parallel diffusivity and fractional anisotropy in the corpus callosum, anterior commissure, and internal capsule were related to the increased presence of activated microglial cells in these regions; the e_1 and fractional anisotropy were compared against the ratio of activated microglial cells to the total number of microglial cells in all 3 regions for the control and endotoxin kits (Figure 5). A decrease in e_1 and fractional anisotropy with increase in the proportion of activated microglial cells is seen in all 3 regions, with a clear separation between the control and the endotoxin groups.

Although a negative correlation was seen for e_1 and fractional anisotropy when compared with proportion of activated microglia, it is possible that some of this difference may be due to the significant difference in the mean values of these parameters between the groups. Nevertheless, it does appear that the decrease in e_1 and fractional anisotropy in the corpus callosum, anterior commissure, and internal capsule of the endotoxin kits is related to the increased presence of activated microglial cells in these regions at this age. A correlation was not noted between increase in activated microglia and change in apparent diffusion coefficient or e_{23} for these regions. This indicates that the changes in diffusivity in the white matter regions may be related to the presence of neuroinflammation and infiltration by microglial cells in the endotoxin kits.

Newborn brain sections, when stained with pan-axonal neurofilament marker SMI-312, which immunolabels complex networks of axons and is directed against highly phosphorylated axonal epitopes of neurofilaments,[20,24] showed no difference in the immunoreactivity for phosphorylated neurofilament in the periventricular white matter regions between the endotoxin and the control groups, indicating that an obvious decrease in number of axons was not noted at this stage (Figure 6).

Discussion

In this study, we have used diffusion tensor imaging to noninvasively evaluate the effect of the presence of neuroinflammation induced by intrauterine endotoxin administration on water diffusivity changes in the white matter of newborn rabbits. A decrease in parallel diffusivity along with a decrease in the fractional anisotropy is demonstrated in the white matter regions. This may be related to the increased presence of activated microglia and astrocytes in these regions. We have previously shown in this model that intrauterine injection of endotoxin near-term leads to microglial activation in the neonatal brain that can be detected by positron emission tomography (PET) using the tracer ^{11}C-(*R*)-PK11195, and motor deficits in newborn rabbit.[21,22] Our results did not show an obvious decrease in staining of phosphorylated neurofilaments in the periventricular white matter regions of newborn rabbit after maternal endotoxin administration. However, a robust activation of microglial cells and astrocytes was observed in these regions. These findings suggest that in our model, the decrease in e_1 resulting in a decrease in fractional anisotropy could be explained by the presence of activated microglia and astrocytes in white matter regions of endotoxin kits.

Diffusion tensor imaging has been widely used to detect white matter injury in animal models of multiple sclerosis,[25] spinal cord injury,[26,27] ischemia,[28,29] and with cuprizone instillation.[30,31] These studies have shown a correlation between the directional diffusivities and the histological findings. A decrease in e_1 appears to be associated with axonal damage, whereas an increase in e_{23} is associated with myelin injury. Although myelin plays a role in anisotropy, it appears not to be an essential component for anisotropic diffusion in neural fibers.[32] Structural features of the axons other than myelin appear to be a significant source of anisotropy.[32] Harsan and colleagues have used in vivo diffusion tensor imaging to characterize the brain white matter tracts in a mouse model of Pelizaeus-Merzbacher disease, where an irreversible dysmyelination is accompanied by oligodendrocyte death and astrocyte hypertrophy.[33] The authors suggested that the increase in parallel and perpendicular diffusivity noted in these animals may be related to the hypertrophic astrocytes that wrapped around and tended to run parallel to the long axis of the unmyelinated axons. However, in our model a decrease in parallel diffusivity is noted, which may be because of the infiltration of activated microglial cells that are typically enlarged and rounded in shape without long processes and ramifications. The presence of these micro-glial cells in the white matter regions may decrease the parallel diffusion normally seen along the axons. Although an obvious decrease in neurofilament staining is not seen in these regions, the presence of axonal disorganization and/or damage cannot be ruled out because there is a tendency toward an increase in the perpendicular diffusivity in our model in these regions. This may explain the presence of motor deficits in our model and the hypomyelination observed on histology at postnatal day 5.[22]

In addition to the changes in water diffusivity in the white matter, a decrease in e_1 and e_{23} followed by a decrease in apparent diffusion coefficient without change in fractional anisotropy was noted in the hippocampus in the endotoxin-exposed kits. This decrease in diffusion in the hippocampus may be related to the swelling of astrocytes and/or microglial activation, increasing the local cellularity in these regions. Similar findings have been

reported in a rat model of middle cerebral artery stroke, where a decrease in diffusion with increase in cellular swelling was noted in the ipsilateral substantia nigra.[34] In patients with middle cerebral artery infarct, a decrease in diffusion in ipsilateral thalamus was thought to be related to microglial activation in this region.[35]

Using a rabbit model of intrauterine hypoxic-ischemic injury, Drobyshevsky and colleagues examined white matter injury by diffusion tensor imaging. An increase in e_{23} resulting in a decrease in fractional anisotropy was observed in the periventricular white matter of hypertonic newborn rabbits at postnatal day1. In these kits, there was no change in e_1 in white matter regions. These diffusion tensor imaging findings were accompanied by a decrease in white matter volume and a loss of immunoreactivity for phosphorylated neurofilaments in the white matter. The authors suggested that the disruption of structural organization of white matter in hypertonic kits may be explained by initial injury to oligodendroglia after hypoxia-ischemia.[36] The discrepancy between the diffusion tensor imaging and the immunohistochemical findings in the hypoxicischemic model and ours could be linked to the timing of the insult in relationship to the fetal brain development. In the hypoxic-ischemic model, hypoxia was induced at E22, a time that correspond to the presence of preoligodendrocytes that have been reported to be vulnerable to hypoxia-ischemia.[37],[38] In our model, lipopolysaccharide injection was performed at E28, a time that correspond to peak of microglial cell density in white matter tracts of rabbit.[39] Hence in our model, at postnatal day 1 the presence of gliosis may contribute the most toward the changes in diffusivity, resulting in a decrease in the parallel diffusivity. This intense microglial infiltration may overwhelm diffusivity changes due to axonal disruption or loss of structural organization. This hypothesis can be verified by longitudinal studies using diffusion tensor imaging and immunohistochemical techniques to evaluate the effect of activated microglia and astrocytes on axonal and myelin integrity.

In the current study, the decrease in fractional anisotropy observed in periventricular white matter of endotoxin newborn rabbits seems mainly due to the decrease in e_1. The tendency toward an increase in e_{23} noted in corpus callosum, internal capsule, and corona radiata that becomes significant in the anterior commissure could also contribute to the decrease in fractional anisotropy in these regions of the endotoxin rabbits. The inability to detect significant changes in e_{23} could be explained by the immaturity of rabbit white matter at an early postnatal age. The myelination in rabbit is similar to that of human brain because it occurs in the perinatal period. In rabbit, myeli-nation begins in the internal capsule at postnatal day 5 and in the corpus callosum at postnatal day 11. At postnatal day 11, intense myelination was present in the rabbit white matter regions, including internal capsule, corona radiata, and anterior commissure.[36] In humans, myelination begins in late fetal development and during the early postnatal period and is more active during the first year after birth.[40],[41] Hence, the premyelinating state of the white matter tract in the newborn rabbit could contribute to the moderate change in e_{23} in corpus callosum, internal capsule, and corona radiata regions. In the endotoxin rabbits, the decrease in parallel diffusivity with little increase in the perpendicular diffusivity suggests that at postnatal day 1, the effect of the presence of activated microglia and astrocytes is more dominant than the effect of absence or loss of myelin on this directional diffusivity. Changes in diffusivity that are more characteristic of axonal injury and myelin loss may be more obvious at later ages beyond the time period of peak microglial activation.

The observed decrease in fractional anisotropy in our study is consistent with reported diffusion tensor imaging findings in clinical studies. A decrease in fractional anisotropy with no change in apparent diffusion coefficient was noted in the cervical cord of patients with amyotrophic lateral sclerosis[42] and in periventricular white matter of neonates with meningitis.[43] Because diffuse astrocytosis and microglial activation are a common finding in

multiple sclerosis,[44] amyotrophic lateral sclerosis,[45] and infection,[46] the authors suggested that the decrease in fractional anisotropy could be related in part to the presence of reactive gliosis. Diffusion tensor imaging studies of infants with periventricular leukomalacia and cerebral palsy have demonstrated a decrease in fractional anisotropy in the affected white matter regions that may be accompanied by an increase in apparent diffusion coefficient, but the changes in diffusion tensor imaging-derived parameters including e_1 and e_{23} have not been detailed.[12,13,15,47,48] A decrease in fractional anisotropy with no change in apparent diffusion coefficient was seen in term infants with moderate hypoxic-ischemic injury and was thought to be a more sensitive indicator of injury.[49] Arzoumanian and colleagues found that a decrease in fractional anisotropy in the internal capsule in preterm infants correlated with development of abnormal neurolologic outcomes, including cerebral palsy at 18 months to 24 months of age.[47] In a recent study using diffusion tensor imaging fiber-tracking techniques to evaluate sensoriomotor fibers in patients with periventricular leukomalacia, the authors reported a decrease in fractional anisotropy in infants 9 months to 41 months of age, which correlated with motor disabilities characterized by cerebral palsy at 15 months to 63 months.[50] Taken together, these findings and our results suggest that diffusion tensor imaging may be a useful noninvasive tool in evaluating neuroinflammation and white matter injury soon after birth and in predicting neurological abnormalities in infants who have been exposed to intrauterine infection. In addition, it would be important to take into account the timing of exposure to the inflammatory stimulus in relation to the presence of microglia in white matter tracts, to determine the nature and the degree of white matter injury in fetuses exposed to chorioamnionitis. Peak microglial activation is known to occur 48 to 72 hours after the inflammatory stimulus.[51] Hence, at postnatal day 1, the effect of micro-glial activation may be the most dominant contributor to change in diffusivity in this model.

In summary, this study demonstrates that intrauterine injection of endotoxin near-term leads to water diffusivity changes in periventricular white matter of newborn rabbits that can be detected noninvasively by diffusion tensor imaging. Our data suggest that these changes in water diffusivity may be explained in part by the infiltration of activated microglia and astrocytes in the periventricular white matter of postnatal day 1 rabbits exposed to maternal inflammation in utero. Longitudinal diffusion tensor imaging studies and immunohistochemical analyses will help delineate the relative contributions of gliosis versus axonal damage and dysmyelination in changes in diffusivity in maternal inflammation-induced perinatal brain injury.

Acknowledgments

This research was supported (in part) by the Perinatology Research Branch, Division of Intramural Research, Eunice Kennedy Shriver National Institute of Child Health and Human Development, National Institutes of Health (NIH), Department of Health and Human Services and by 5K08HD050652, National Institute of Child Health and Human Development. This research was presented at the Neurobiology of Disease in Children Conference: Symposium on Injury to the Preterm Brain and Cerebral Palsy, in conjunction with the 37th Annual Meeting of the Child Neurology Society, Santa Clara, California, November 5, 2008. This work was supported by grants from the NIH (5R13NS040925-09), the Cerebral Palsy International Research Foundation, the Kennedy Krieger Institute, and the Child Neurology Society.

References

1. Dammann O, Leviton A. Maternal intrauterine infection, cytokines, and brain damage in the preterm newborn. Pediatr Res. 1997; 42(1):1–8. [PubMed: 9212029]
2. Goepfert AR, Andrews WW, Carlo W, et al. Umbilical cord plasma interleukin-6 concentrations in preterm infants and risk of neonatal morbidity. Am J Obstet Gynecol. 2004; 191(4):1375–1381. [PubMed: 15507968]

3. Heep A, Behrendt D, Nitsch P, Fimmers R, Bartmann P, Dembinski J. Increased serum levels of interleukin 6 are associated with severe intraventricular haemorrhage in extremely premature infants. Arch Dis Child Fetal Neonatal Ed. 2003; 88(6):501–504.
4. Nelson KB, Dambrosia JM, Grether JK, Phillips TM. Neonatal cytokines and coagulation factors in children with cerebral palsy. Ann Neurol. 1998; 44(4):665–675. [PubMed: 9778266]
5. Viscardi RM, Muhumuza CK, Rodriguez A, et al. Inflammatory markers in intrauterine and fetal blood and cerebrospinal fluid compartments are associated with adverse pulmonary and neurologic outcomes in preterm infants. Pediatr Res. 2004; 55(6):1009–1017. [PubMed: 15155869]
6. Yoon BH, Jun JK, Romero R, et al. Amniotic fluid inflammatory cytokines (interleukin-6, interleukin-1beta, and tumor necrosis factor-alpha), neonatal brain white matter lesions, and cerebral palsy. Am J Obstet Gynecol. 1997; 177(1):19–26. [PubMed: 9240577]
7. Yoon BH, Romero R, Park JS. Fetal exposure to an intra-amniotic inflammation and the development of cerebral palsy at the age of three years. Am J Obstet Gynecol. 2000; 182(3):657–681.
8. Cioni G, Di Paco MC, Bertuccelli B, Paolicelli PB, Canapicchi R. MRI findings and sensoriomotor development in infants with bilateral spastic cerebral palsy. Brain Dev. 1997; 19(4):245–253. [PubMed: 9187473]
9. Hashimoto K, Hasegawa H, Kida Y, Takeuchi Y. Correlation between neuroimaging and neurological outcome in periventricular leukomaleacia: diagnostic criteria. Pediatr Int. 2001; 43(3): 240–245. [PubMed: 11380916]
10. Kulak W, Sobaniec W, Kubas B, et al. Spastic cerebral palsy: clinical magnetic resonance imaging correlation of 129 children. J Child Neurol. 2007; 22(1):8–14. [PubMed: 17608298]
11. Kwong KL, Wong YC, Fong CM, Wong SN, So KT. Magnetic resonance imaging in 122 children with spastic cerebral palsy. Pediatr Neurol. 2004; 31(3):172–176. [PubMed: 15351015]
12. Lee ZI, Byun WM, Jang SH, Ahn SH, Moon HK, Chang Y. Diffusion tensor magnetic resonance imaging of microstructural abnormalities in children with brain injury. Am J Phys Med Rehabil. 2003; 82(7):556–559. [PubMed: 12819543]
13. Son SM, Ahn YH, Sakong J, et al. Diffusion tensor imaging demonstrates focal lesions of the corticospinal tract in hemiparetic patients with cerebral palsy. Neurosci Lett. 2007; 420(1):34–38. [PubMed: 17512661]
14. Korzeniewski SJ, Birbeck G, DeLano MC, Potchen MJ, Paneth N. A systematic review of neuroimaging for cerebral palsy. J Child Neurol. 2008; 23(2):216–227. [PubMed: 18263759]
15. Fan GG, Yu B, Quan SM, Sun BH, Guo QY. Potential of diffusion tensor MRI in the assessment of periventricular leukomalacia. Clin Radiol. 2006; 61(4):358–364. [PubMed: 16546466]
16. Neil J, Miller J, Mukherjee P, Hüppi PS. Diffusion tensor imaging of normal and injured developing human brain-a technical review. NMR Biomed. 2002; 15(7-8):543–552. [PubMed: 12489100]
17. Drobyshevsky A, Bregman J, Storey P, et al. Serial diffusion tensor imaging detects white matter changes that correlate with motor outcome in premature infants. Dev Neurosci. 2007; 29(4-5): 289–301. [PubMed: 17762197]
18. Ådén U, Dahlberg V, Fredholm BB, Lai LJ, Chen Z, Bjelke B. MRI Evaluation and functional assessment of brain injury after hypoxic ischemia in neonatal mice. Stroke. 2002; 33(5):1405–1410. [PubMed: 11988622]
19. Rumpel H, Nedelcu J, Aguzzi A, Martin E. Late glial Swelling after acute cerebral hypoxia-ischemia in the neonatal rat: a combined magnetic resonance and histochemical study. Pediatr Res. 1997; 42(1):54–59. [PubMed: 9212037]
20. Drobyshevsky A, Derrick M, Wyrwicz AM, et al. White matter injury correlates with hypertonia in an animal model of cerebral palsy. J Cereb Blood Flow Metab. 2007; 27(2):270–281. [PubMed: 16736047]
21. Kannan S, Saadani-Makki F, Muzik O, et al. Microglial activation in perinatal rabbit brain induced by intrauterine inflammation: detection with 11C-(R)-PK11195 and small-animal PET. J Nucl Med. 2007; 48(6):946–954. [PubMed: 17504871]

22. Saadani-Makki F, Kannan S, Lu X, et al. Intrauterine administration of endotoxin leads to motor deficits in a rabbit model: a link between prenatal infection and cerebral palsy. Am J Obstet Gynecol. 2008; 199(6):651–657. [PubMed: 18845289]
23. Jiang H, van Zijl PC, Kim J, Pearlson GD, Mori S. DtiStudio: resource program for diffusion tensor computation and fiber bundle tracking. Comput Methods Programs Biomed. 2006; 81(2): 106–116. [PubMed: 16413083]
24. Ulfig N, Nickel J, Bohl J. Monoclonal antibodies SMI 311 and SMI 312 as tools to investigate the maturation of nerve cells and axonal patterns in human fetal brain. Cell Tissue Res. 1998; 291(3): 433–443. [PubMed: 9477300]
25. Sun SW, Liang HF, Schmidt RE, Cross AH, Song SK. Selective vulnerability of cerebral white matter in a murine model of multiple sclerosis detected using diffusion tensor imaging. Neurobiol Dis. 2007; 28(1):30–38. [PubMed: 17683944]
26. Budde MD, Kim JH, Liang HF, et al. Toward accurate diagnosis of white matter pathology using diffusion tensor imaging. Magn Reson Med. 2007; 57(4):688–695. [PubMed: 17390365]
27. Kim JH, Loy DN, Liang HF, Trinkaus K, Schmidt RE, Song SK. Noninvasive diffusion tensor imaging of evolving white matter pathology in a mouse model of acute spinal cord injury. Magn Reson Med. 2007; 58(2):253–260. [PubMed: 17654597]
28. Sun SW, Liang HF, Cross AH, Song SK. Evolving Wallerian degeneration after transient retinal ischemia in mice characterized by diffusion tensor imaging. NeuroImage. 2008; 40(1):1–10. [PubMed: 18187343]
29. Sun SW, Liang HF, Le TQ, Armstrong RC, Cross AH, Song SK. Differential sensitivity of in vivo and ex vivo diffusion tensor imaging to evolving optic nerve injury in mice with retinal ischemia. NeuroImage. 2006; 32(3):1195–1204. [PubMed: 16797189]
30. Song SK, Yoshino J, Le TQ, et al. Demyelination increases radial diffusivity in corpus callosum of mouse brain. NeuroImage. 2005; 26(1):132–140. [PubMed: 15862213]
31. Sun SW, Liang HF, Trinkaus K, Cross AH, Armstrong RC, Song SK. Noninvasive detection of cuprizone induced axonal damage and demyelination in the mouse corpus callosum. Magn Reson Med. 2006; 55(2):302–308. [PubMed: 16408263]
32. Beaulieu C. The basis of anisotropic water diffusion in the nervous system—a technical review. NMR Biomed. 2002; 15(7-8):435–455. [PubMed: 12489094]
33. Harsan LA, Poulet P, Guignard B, Parizel N, Skoff RP, Ghandour MS. Astrocytic hypertrophy in dysmyelination influences the diffusion anisotropy of white matter. J Neurosci Res. 2007; 85(5): 935–944. [PubMed: 17278151]
34. Nakane M, Tamura A, Miyasaka N, Nagaoka T, Kuroiwa T. Astrocytic swelling in the ipsilateral substantia nigra after occlusion of the middle cerebral artery in rats. AJNR Am J Neuroradiol. 2001; 22(4):660–663. [PubMed: 11290474]
35. Hervé D, Molko N, Pappata S, et al. Longitudinal thalamic diffusion changes after middle cerebral artery infarcts. J Neurol Neurosurg Psychiatry. 2005; 76(2):200–205. [PubMed: 15654032]
36. Drobyshevsky A, Song SK, Gamkrelidze G, et al. Developmental changes in diffusion anisotropy coincide with immature oligodendrocyte progression and maturation of compound action potential. J Neurosci. 2005; 25(25):5988–5997. [PubMed: 15976088]
37. Back SA, Luo NL, Borenstein NS, Levine JM, Volpe JJ, Kinney HC. Late oligodendrocytes progenitors coincide with the developmental window of vulnerability for human perinatal white matter injury. J Neurosci. 2001; 21(4):1302–1312. [PubMed: 11160401]
38. Back SA, Han BH, Luo NL, et al. Selective vulnerability of late oligodendrocyte progenitors to hypoxia-ischemia. J Neurosci. 2002; 22(2):455–463. [PubMed: 11784790]
39. Bass WT, Singer GA, Liuzzi FJ. Transient lectin binding by white matter tract border zone microglia in the foetal rabbit brain. Histochem J. 1998; 30(9):657–666. [PubMed: 9870766]
40. de Graaf-Peters VB, Hadders-Algra M. Ontogeny of the human central nervous system: What is happening when? Early Hum Dev. 2006; 82(4):257–266. [PubMed: 16360292]
41. Fields RD. Myelination: an overlooked mechanism of synaptic plasticity? Neuroscientist. 2005; 11(6):528–531. [PubMed: 16282593]

42. Valsasina P, Agosta F, Benedetti B, et al. Diffusion anisotropy of the cervical cord is strictly associated with disability in amyotrophic lateral sclerosis. J Neurol Neurosurg Psychiatry. 2007; 78(5):480–484. [PubMed: 17030586]
43. Malik GK, Trivedi R, Gupta A, Singh R, Prasad KN, Gupta RK. Quantitative DTI assessment of periventricular white matter in neonatal meningitis. Brain Dev. 2008; 30(5):334–341. [PubMed: 18006262]
44. Allen IV, McKeown SR. A histological, histochemical and biochemical study of the macroscopically normal white matter in multiple sclerosis. J Neurol Sci. 1979; 41(1):81–91. [PubMed: 438845]
45. Neusch C, Bähr M, Schneider-Gold C. Glia cells in amyotrophic lateral sclerosis: new clues to understanding an old disease? Muscle Nerve. 2007; 35(6):712–724. [PubMed: 17373702]
46. Nau R, Brück W. Neuronal injury in bacterial meningitis; mechanisms and implications for therapy. Trends Neurosci. 2002; 25(1):38–45. [PubMed: 11801337]
47. Arzoumanian Y, Mirmiran M, Barnes PD, et al. Diffusion tensor brain imaging findings at term-equivalent age may predict neurologic abnormalities in low birth preterm infants. AJNR Am J Neuroradiol. 2003; 24(8):1646–1653. [PubMed: 13679287]
48. Thomas B, Eyssen M, Peeters R, et al. Quantitative diffusion tensor imaging in cerebral palsy due to periventricular white matter injury. Brain. 2005; 128(pt 11):2562–2577. [PubMed: 16049045]
49. Ward P, Counsell S, Allsop J, et al. Reduced fractional anisotropy on diffusion tensor magnetic resonance imaging after hypoxicischemic encephalopathy. Pediatrics. 2006; 117(4):619–630.
50. Murakami A, Morimoto M, Yamada K, et al. Fiber tracking techniques can predict the degree of neurologic impairment for periventricular leukomalacia. Pediatrics. 2008; 122(3):500–506. [PubMed: 18762518]
51. Herber DL, Maloney JL, Roth LM, Freeman MJ, Morgan D, Gordon MN. Diverse microglial responses after intrahippocampal administration of lipopolysaccharide. Glia. 53(4):382–391. 200. [PubMed: 16288481]

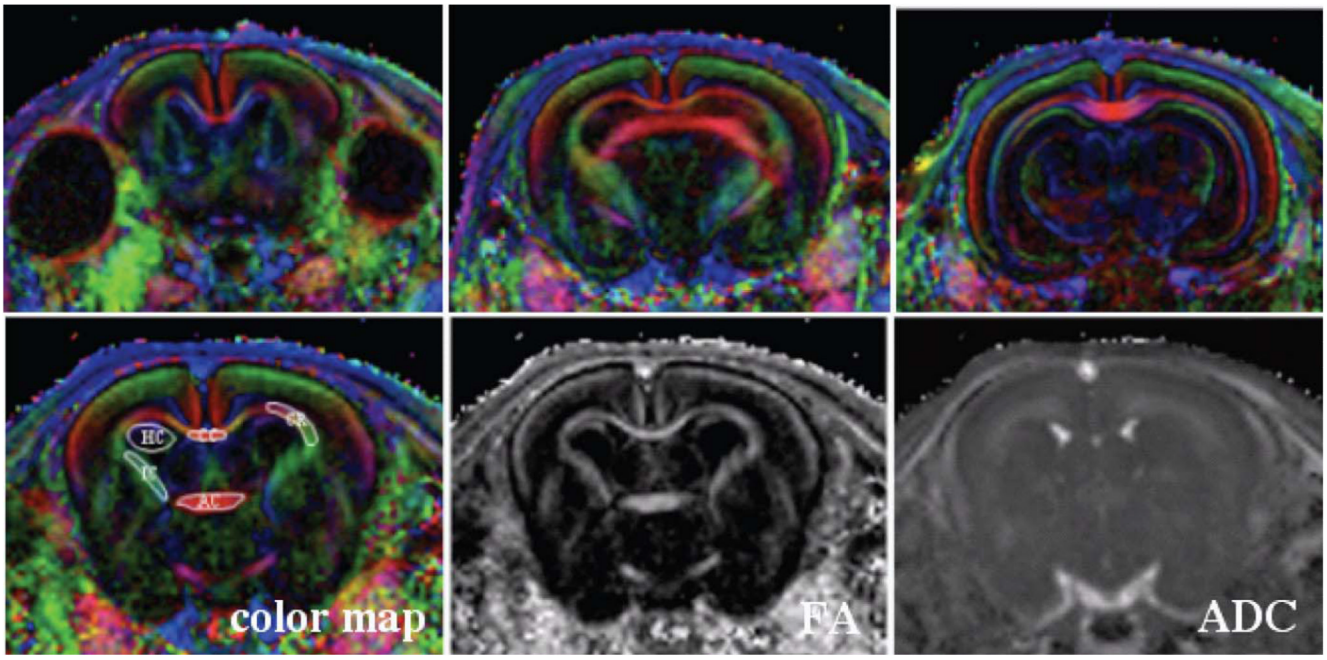

Figure 1.

Representative color-encoded maps (upper row) as well as the resulting fractional anisotrophy and apparent diffusion coefficient maps (bottom row) obtained from a control postnatal day 1 rabbit kit. Eight contiguous coronal images with slice thickness of 0.7 and 0.25 mm in plane each were acquired, starting from the level of the bregma. Fibers that are oriented left-right are encoded in red, those that are oriented dorsoventral are encoded in green, and those oriented craniocaudal are encoded in blue color. The regions of interest were manually drawn in the corpus callosum, internal capsule, corona radiata, anterior commissure, and hippocampus (bottom row left) and subsequently transferred to the fractional anisotrophy and apparent diffusion coefficient maps. ADC, apparent diffusion coefficient.

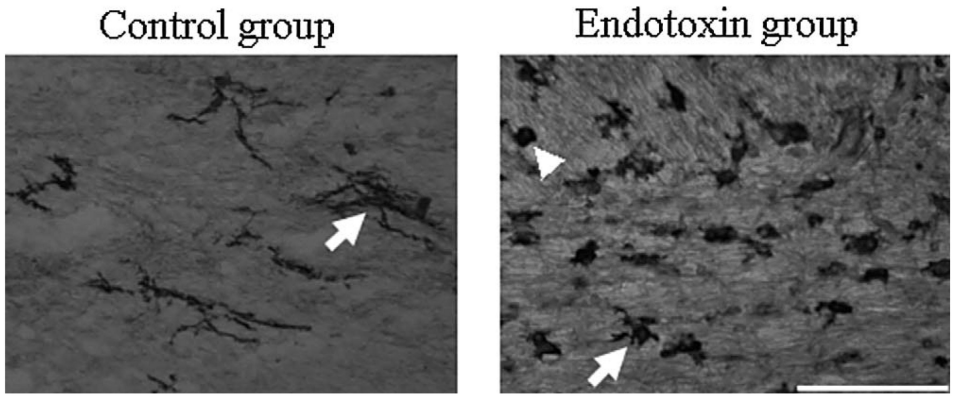

Figure 2.
Morphology of microglial cells using tomato lectin staining. Arrows indicate microglial cells that are highly ramified in the control group and become less ramified, bushy (arrow), and rounded (indicated by arrowhead) in the endotoxin group. This change in the morphology is accompanied by an increase in the density of microglial cells. Scale bar = 100 μm.

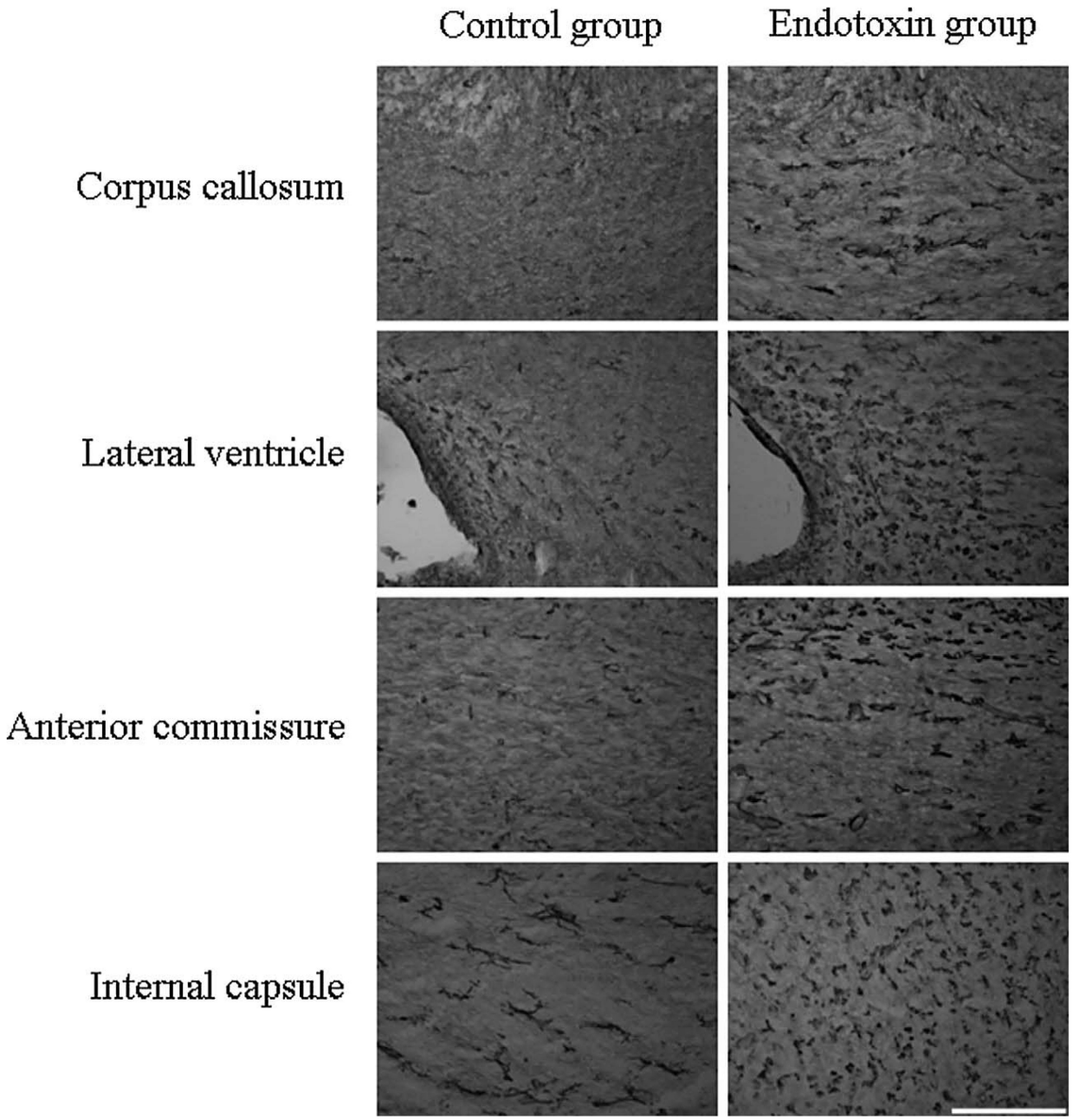

Figure 3.
Microglial cells staining in periventricular white matter regions. Brain sections from postnatal day 1 control and endotoxin rabbits were stained for microglial cells using tomato lectin. An increase in activated microglial cells along with change in the morphology from ramified cells to bushy and round cells are noted in the endotoxin kits when compared to the control kits in the regions of the corpus callosum, along the lateral ventricle, anterior commissure, and the internal capsule. Scale bar = 200 μm.

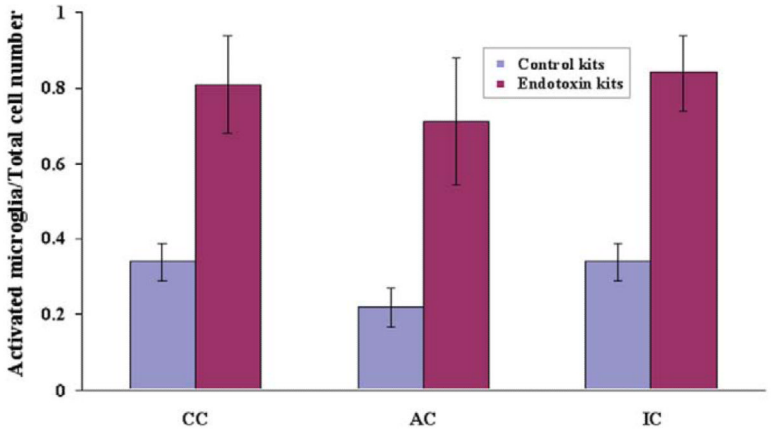

Figure 4.

Ratio of activated microglial cells compared to the total number of microglia in the corpus callosum, anterior commissure, and internal capsule. A significant increase in the ratio of activated to total number of microglial cells indicating significant neuroinflammation in these regions was seen in the endotoxin kits compared with controls at postnatal day 1 (Data represented as mean ± SD). AC, anterior commissure; CC, corpus callosum; IC, internal capsule.

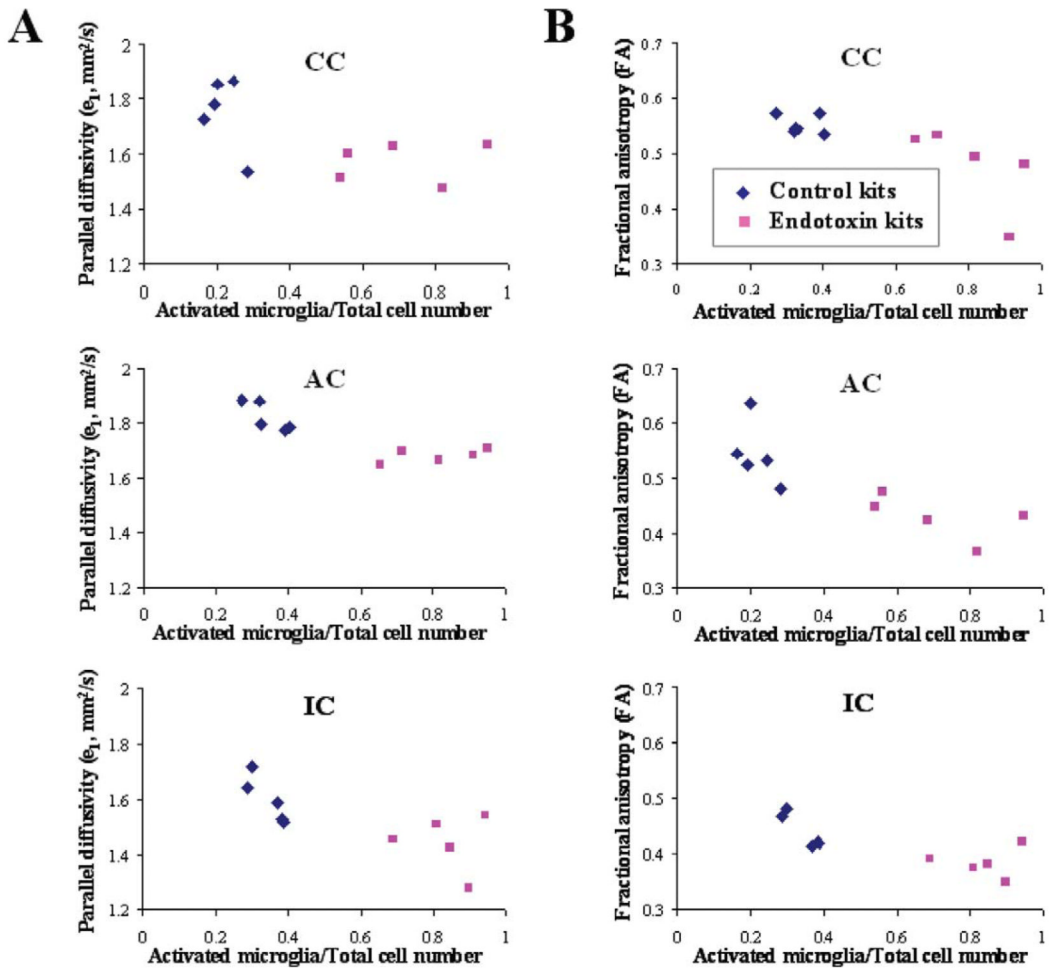

Figure 5.

Ratio of activated cells to total number of microglial cells plotted against parallel diffusivity and fractional anisotropy. Scatter plot of ratio of activated to total microglial cells versus e_1 (A) and fractional anisotrophy (B) in corpus callosum, anterior commissure, and internal capsule. Each symbol represents data from 1 rabbit kit for the indicated region. An increase in the proportion of activated microglia is associated with a decrease in parallel diffusivity (R = .70, .52, and .40 for the corpus callosum, internal capsule, and anterior commissure, respectively) and a decrease in fractional anisotropy (R = .57, .57, and .69 for the corpus callosum, internal capsule, and anterior commissure, respectively). This indicates that the decrease in parallel diffusivity and fractional anisotropy in the endotoxin kits may be related to the increased presence of activated microglia in these regions. AC, anterior commissure; CC, corpus callosum; IC, internal capsule.

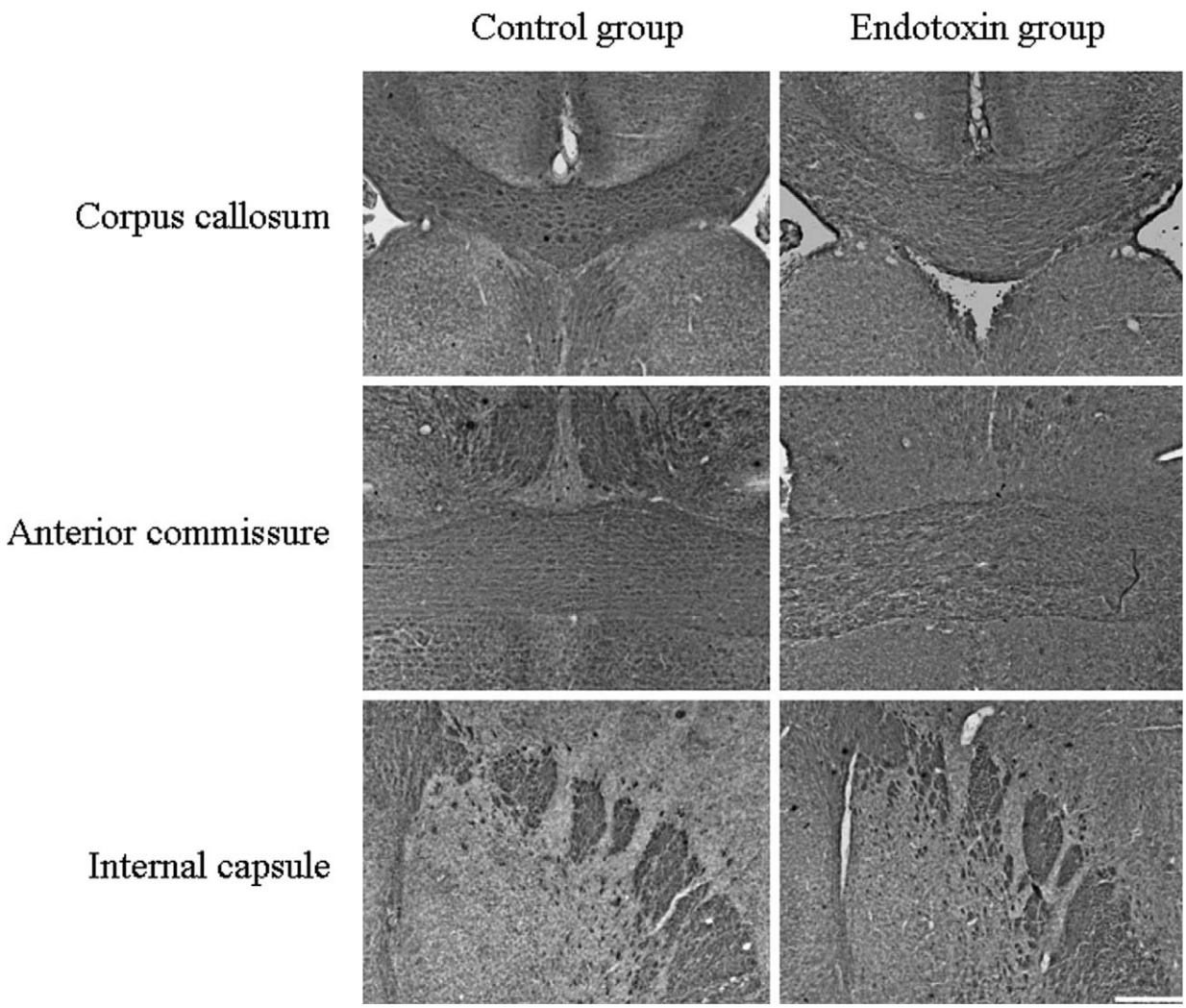

Figure 6.

Staining for phosphorylated neurofilaments. Brain sections from postnatal day 1 control and endotoxin rabbits were stained for phosphorylated neurofilament using pan-axonal neurofilament marker SMI-312. There is no obvious decrease in the immunoreactivity for phosphorylated neurofilaments noted in the endotoxin kits compared with controls at postnatal day 1. Scale bar = 200 μm.

Table 1

Diffusion Tensor Parameter Values in Selected Regions of Interest of Control and Endotoxin Rabbit Kits at Postnatal Day 1[a]

ROIs	Group	e_1 (10^{-3} mm^2/s)	e_{23} (10^{-3} mm^2/s)	ADC (10^{-3} mm^2/s)	FA
Corpus callosum	Control	1.81 (1.78-1.84)	0.68 (0.64-0.71	1.06 (1.03-1.08)	0.56 (0.55-0.57)
	Endotoxin	1.68[c] (1.66-1.70)	0.76 (0.66-0.87)	1.07 (0.99-1.14)	0.48[b] (0.42-0.54)
Anterior commissure	Control	1.76 (1.67-1.84)	0.69 (0.67-0.72)	1.05 (1.01-1.08)	0.54 (0.51-0.58)
	Endotoxin	1.57[c] (1.52-1.63)	0.78[c] (0.73-0.82)	1.04 (1.00-1.08)	0.43[c] (0.40-0.46)
Internal capsule	Control	1.56 (1.52-1.61)	0.74 (0.71-0.77)	1.02 (0.99-1.04)	0.44 (0.42-0.46)
	Endotoxin	1.44[c] (1.35-1.52)	0.77 (0.74-0.79)	0.99 (0.95-1.03	0.38[c] (0.36-0.40)
Corona radiata	Control	1.72 (1.69-1.75)	0.86 (0.81-0.91)	1.15 (1.11-1.19)	0.42 (0.39-0.45)
	Endotoxin	1.66[b] (1.62-1.70)	0.91 (0.86-0.96)	1.16 (1.12-1.20	0.37[b] (0.35-0.39)
Hippocampus	Control	1.55 (1.40-1.69)	1.18 (1.10-1.25)	1.30 (1.20-1.40)	0.18 (0.16-0.21)
	Endotoxin	1.35[b] (1.28-1.43)	1.00[c] (0.96-1.04)	1.12[c] (1.07-1.17)	0.20 (0.18-0.23)

Note: ADC, apparent diffusion coefficient; FA, fractional anisotropy; ROIs, regions of interest.

[a] Values are mean with (95% confidence interval).

[b] $P < .05$

[c] $P < .005$ when compared with controls.

J Child Neurol. Author manuscript; available in PMC 2013 June 13.